Adv Biochem Eng Biotechnol (2016) 152: 35–51
DOI 10.1007/10_2014_274

Published Online: 15 July 2014

Novel Hydrogen Bioreactor and Detection Apparatus

Joseph A. Rollin, Xinhao Ye, Julia Martin del Campo, Michael W. W. Adams and Y.-H. Percival Zhang

Abstract In vitro hydrogen generation represents a clear opportunity for novel bioreactor and system design. Hydrogen, already a globally important commodity chemical, has the potential to become the dominant transportation fuel of the future. Technologies such as in vitro synthetic pathway biotransformation (SyPaB)—the use of more than 10 purified enzymes to catalyze unnatural catabolic pathways—enable the storage of hydrogen in the form of carbohydrates. Biohydrogen production from local carbohydrate resources offers a solution to the most pressing challenges to vehicular and bioenergy uses: small-size distributed production, minimization of CO_2 emissions, and potential low cost, driven by high yield and volumetric productivity. In this study, we introduce a novel bioreactor that provides the oxygen-free gas phase necessary for enzymatic hydrogen generation while regulating temperature and reactor volume. A variety of techniques are currently used for laboratory detection of biohydrogen, but the most information is provided by a continuous low-cost hydrogen sensor. Most such systems currently use electrolysis for calibration; here an alternative method, flow calibration, is introduced. This system is further demonstrated here with the conversion of glucose to hydrogen at a high rate, and the production of hydrogen from glucose 6-phosphate at a greatly increased reaction rate, 157 mmol/L/h at 60 °C.

J. A. Rollin · X. Ye · J. M. del Campo · Y.-H. P. Zhang (✉)
Biological Systems Engineering Department, Virginia Tech, 304 Seitz Hall, Blacksburg, VA 24061, USA
e-mail: ypzhang@vt.edu

J. A. Rollin · Y.-H. P. Zhang
Cell Free Bioinnovations Inc, Blacksburg, VA 24060, USA

J. A. Rollin · Y.-H. P. Zhang
Gate Fuels Inc, Blacksburg, VA 24060, USA

M. W. W. Adams
Department of Biochemistry and Molecular Biology, University of Georgia, Athens, GA 30602, USA

Keywords Biohydrogen · In vitro synthetic biosystem for biomanufacturing · Synthetic pathway biotransformation · Hydrogen bioreactor · Continuous hydrogen detection

Contents

1 Introduction

Hydrogen is currently an important commodity chemical. With a global annual market volume of approximately 45 million metric tons per year and a steady increase in demand over the last three decades [1], hydrogen is used in oil refining, fertilizer (ammonia) production, food production, metal treatment, as rocket engine fuel, as electric generator coolant, and for many other industrial purposes [2]. In addition, hydrogen is a target fuel: it is the energy carrier of the hydrogen economy, a vision that seeks to increase transportation energy efficiency greatly, mitigate non-point source pollution, and minimize greenhouse gas emissions [3, 4].

Because the current market for hydrogen primarily serves the petroleum refining and chemical processing industries, 85 % of hydrogen is used near its production site [5]. For such captive markets, large-scale production by steam–methane reforming (SMR) is by far the most economical method. Accordingly, SMR, a process that generates fossil CO_2 emissions as well as carbon monoxide contaminants, currently accounts for approximately 90 % of hydrogen production [6]. For future use as a fuel, important goals include high purity, distributed hydrogen generation, and maximal use of CO_2-free technologies [3]. Purity is especially important, as proton exchange membrane (PEM) fuel cells are poisoned by carbon monoxide. Biohydrogen made from carbohydrates has the potential to meet these requirements.

Biohydrogen is available from several biological routes. Microbial production options include dark fermentation by a pure microorganism and consortia (combining strains specializing in photosynthesis and fermentation), biophotolysis of water, and photodegradation of organic compounds [7]. Systems incorporating photosynthesis are typically limited by the low energy concentration of solar energy and coproduction of oxygen, which inhibits hydrogenase enzymes. Both of these factors result in low volumetric hydrogen productivity [6]. An advanced, porous glass-immobilized cell reactor achieved rates an order of magnitude higher than other studies [8], but scaling and process economics remain a challenge for such designs. Biohydrogen produced via dark fermentation is more promising, but the maximum theoretical yield is 4 mol H_2/mol hexose (the Thauer limit), making cost effectiveness difficult due to the substrate cost when using media containing carbohydrates [9]. Wastewater treatment solves the substrate cost issue, but introduces other challenges, such as coproduction of other products, such as methane and organic acids.

Microbial hydrogen bioreactors are multiphase by nature, incorporating solid-phase reactants, liquid-phase biocatalysts, and gas-phase products. Continuous operation is usually chosen for applications larger than lab scale, often by using continuously stirred tank reactors (CSTRs), although also packed bed, fluidized bed, or membrane reactors have been used in order to reduce hydraulic residence time, a strategy used to prevent the growth of methanogenic organisms [10, Oh, 2004 #336]. Other challenges for large-scale microbial hydrogen production include oxygen inhibition, mixing, and product inhibition. Oxygen inhibition is solved differently by different organisms: some are able to compartmentalize their hydrogenase enzymes, whereas others are strict anaerobes. In either case, minimal oxygen is desired in the fermentation broth. With typical CSTR mixing, substrate addition results in a highly dynamic environment for the cells, with a wide range of concentration throughout the fermentation broth [11]. Hydrogen and CO_2 are gases, which will bubble out of the fermentation above a certain concentration. However, even low levels of dissolved hydrogen can cause problems for most biohydrogen production systems. Solutions to this problem include hydrogen absorption, stripping by elevated reaction temperature, stripping with a gas, and stripping by evaporation or boiling [12], as well as selective permeable membranes. Each of these options increases the cost of the microbial hydrogen-producing bioreactor.

A solution to some of the complexities of microorganisms is to use instead enzymes to catalyze the reaction from carbohydrate substrates directly. This concept was first pioneered by Woodward [13, 14], who demonstrated the conversion of glucose and glucose 6-phosphate to hydrogen using first two, then eleven enzymes (respectively), and Zhang [15], who enabled the use of a lower-cost substrate, starch. This later discovery, of enzymatic oxidation of a nonphosphorylated substrate completely to hydrogen and CO_2, opened up the possibility of economical large-scale enzymatic hydrogen production. Referred to as a synthetic pathway biotransformation (SyPaB), this technology combines purified enzymes from a variety of different hosts (including animal, plant, bacterial, and archaeal)

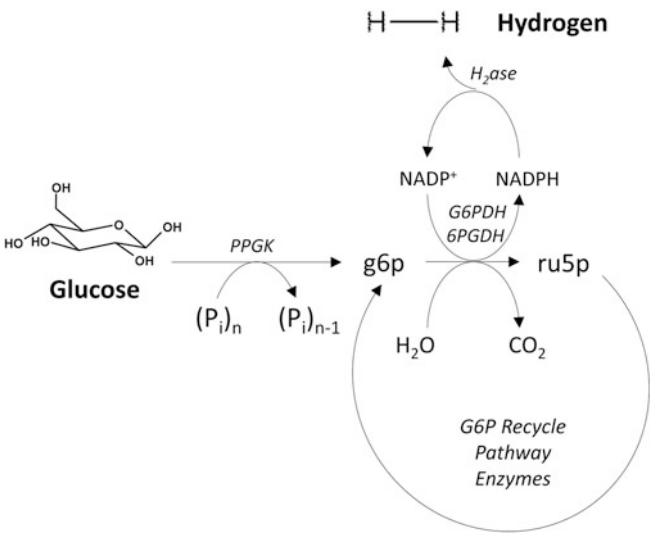

Fig. 1 Synthetic pathway biotransformation (SyPaB) depicting the pathway for conversion of glucose to hydrogen and CO_2. See Rollin et al. [39] for pathways depicting the utilization of additional substrates

to catalyze the high yield of various starting substrates including starch, cello-oligomers, sucrose, and xylose to hydrogen and carbon dioxide. A representative pathway is shown in Fig. 1. This pathway enables production of a 12 mol H_2/mol glucose unit, the theoretical maximum for this molecular conversion and threefold the microbial Thauer limit. Practical yields of over 93 % theoretical have been demonstrated for multiple substrates [16–18]. In this book chapter, the technology features a demonstrated maximum rate of 157 mmol/h/L for the first time, on par with the best biohydrogen rates reported [8].

2 Setup of Hydrogen Production Bioreactor and Detection Apparatus

A system was constructed to study the SyPaB reaction with the following goals: (i) ensure an oxygen-free gas phase in the bioreactor, (ii) remove produced hydrogen with a carrier gas, (iii) ensure constant volume in the bioreactor for long-term operation (preventing evaporative loss or gain of condensation), and (iv) accurately detect a range of hydrogen concentrations, from 1–1,000 ppm, in realtime. A schematic of the system produced is included as Fig. 2a. Our apparatus mimics a similar system at Oak Ridge National Laboratory, which has been described previously in a number of biohydrogen experiments [13, 14, 16, 19–21], with

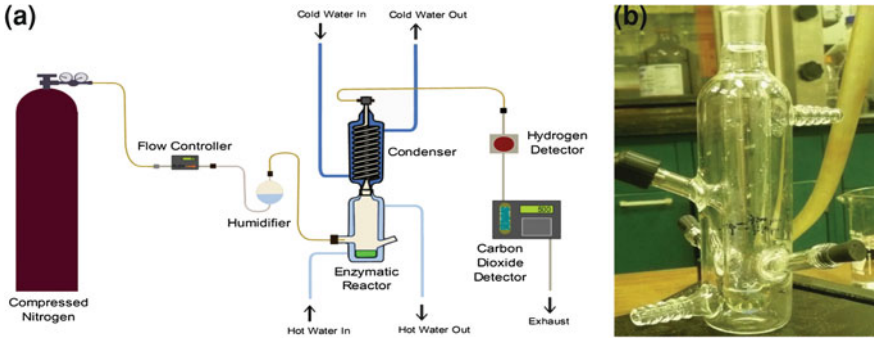

Fig. 2 First-generation, lab-scale hydrogen bioreactor and related hydrogen detection apparatus (**a**). Nitrogen carrier gas is used to prevent oxygen inhibition of hydrogenase. The carrier gas is first humidified before passing through the reactor. A condenser compensates for evaporation of reactor liquid. Hydrogen and carbon dioxide sensors are then used to detect the concentration of these components. The enzymatic reactor (**b**) is a custom glass reactor, which allows temperature control via water bath, carrier gas input, and access to the liquid phase by pipette

some important changes. Specific equipment and software used are summarized in Table 1.

The custom bioreactor designed for this system is shown in Fig. 2b. The reactor is heated with water, warmed in a bath, and pumped through an outer jacket. Actual reactor temperature was found to be 0.4 °C less than the water bath set-point. Gas enters through an upper side port and leaves through the top, where the reactor adjoins a condenser. Lower side injection ports allow addition and removal of the liquid reaction solution, and a stir bar provides sufficient agitation for efficient mass transfer in the system.

In this system, ultra-high–purity (UHP) nitrogen gas is controlled at a rate of 30 mL/min with a gas flow controller (GFC; SKUW-188427, Aalborg, Orangeburg, NY). This carrier gas is first humidified by bubbling through deionized water, after which it enters the reactor. The enzymatic bioreactor is held at a desired temperature (e.g., 50 or 60 °C) with a water jacket and controlled with a water bath (Neslab RTE-7D1, Thermo Scientific, Waltham, MA). Carrier gas plus generated hydrogen and CO_2 next pass through a condenser, held at 21 °C by a second water bath. Condenser temperature was empirically determined to ensure a constant reactor volume. Humidifier, reaction vessel, and condenser were custom fabricated out of borosilicate by the Virginia Tech Department of Chemistry Glass Shop.

Hydrogen detection was conducted using the least costly sensor available, a tin–oxide thermal conductivity detector (TCD) purchased from Figaro (TGS 821, Figaro USA Inc., Glenview, IL). This detector was used as an alternative to simple endpoint gas composition determination by gas chromatography, as is sometimes used in some biohydrogen studies [22, 23]. Such detection methods enable accurate measurement of produced gas, but have the limitations of cost, maintenance, and requiring several minutes per sample, preventing the precise measurement of hydrogen production in systems of quickly changing hydrogen

Table 1 Key hydrogen production and detection apparatus components

Key part	Function	Manufacturer (product name)
Bioreactor	Provide easy access for liquid and solid additions, allow sampling without oxygen introduction, nitrogen-flushed headspace for anaerobic conditions	Virginia Tech department of chemistry (custom glassware)
H_2 detector	Specifically detect hydrogen at concentrations ranging from 1–1000 ppm	Figaro (TGS 821)
Gas flow controller	Ensure steady nitrogen flow rate through system	Aalborg (GFC /SKUW-188427)
Refrigerated water circulator bath	Hold reactor and condenser temperatures steady	Thermo Scientific (Neslab RTE-7D1)
Interface	Convert analog sensor output to digital	National Instruments (USB-6210 DAQ)
LabView software	Continuously log data throughout hydrogen production and calibration experiments	National Instruments (SignalExpress)

production rate. Thermal conductivity is measured in a TCD by comparing the voltage being transmitted across a reference semiconductor with a semiconductor in contact with a sample gas stream. A property of hydrogen gas is extremely high thermal conductivity; this property is used to detect the concentration of hydrogen in the sample stream. A custom aluminum housing for the TCD was manufactured by the Virginia Tech Department of Chemistry. TCD output was routed to a computer for data acquisition using a USB-6210 DAQ (National Instruments, Austin, TX).

As opposed to the ORNL hydrogen detection system, where extensive humidity controls were employed prior to the tin–oxide hydrogen sensor, we found these components to be unnecessary. The key considerations for accurately using a TCD are constant temperature, humidity, and pressure [24]. Constant humidity was maintained by refilling the humidifier before each experiment, and detector temperature was held constant by placing the TCD in an oven held at 44–46 °C. Pressure in the hydrogen sensor is important due to the effect it has on humidity, temperature, and local hydrogen concentration. Here pressure was maintained at slightly below atmospheric by use of a second flow controller at the exhaust.

In similar systems others have employed electrolysis as a means of calibrating the hydrogen detector [14–16, 19, 20]. In this calibration method, a precise current is applied to a Hoffman apparatus or similar electrolysis device, generating H_2 and O_2 from 1 mM KOH. The level of hydrogen detected by TCD may then be calculated by relating the voltage displayed [19]. This method provided consistent results in previous studies, but the accuracy of the electrolysis calculation depends on the accuracy of the assumed faradaic efficiency (not taking into effect inefficiencies caused by the generation of heat and side reactions, including hydrogen

peroxide generation). Because this efficiency is not easily measured, and varies between electrolysis systems, we used a different method: flow calibration.

The flow calibration used serial dilution of a UHP hydrogen stream with UHP nitrogen. A flow diagram of this procedure is shown in Fig. 3. In this example, 2.0 mL/min H_2 is mixed with 200 mL/min N_2 to generate a hydrogen mass fraction of 0.01. A rate of 1 mL/min of this mixture is then again diluted, by the addition of 30 mL/min N_2, resulting in a final hydrogen concentration of 330 ppm. Each of these flow rates was controlled by GFC. Using this method, concentrations from below 10 ppm to over 1 % hydrogen were introduced to the TCD and the output voltage recorded (Fig. 4a). This procedure was repeated, and the results were used to build a calibration curve (Fig. 4b). The flow calibration was repeated bimonthly while experiments were being run. In future experiments where higher than 1 % hydrogen is to be detected, use of an electrochemical sensor from Hach Ultra Analytics (Loveland, CO) is recommended; membrane model 2995A is capable of detecting up to 100 % H_2.

3 Experimental

3.1 Chemicals and Strains

All chemicals were reagent grade and purchased from Sigma-Aldrich (St. Louis, MO) and Fisher Scientific (Pittsburgh, PA), unless otherwise noted. *E. coli* BL21 Star (DE3) (Invitrogen, Carlsbad, CA) containing a protein expression plasmid was used to produce all recombinant protein (enzymes #1–11). Luria-Bertani (LB) medium was used for *E. coli* cell growth and recombinant protein expression supplemented with 100 μg/mL ampicillin or 50 μg/mL kanamycin. Oligonucleotides were synthesized by Integrated DNA Technologies (Coraville, IA) and Fisher Scientific. Hydrogenase SH1 from *Pyrococcus furiosus* was provided by Dr. Michael Adams [25].

3.2 Recombinant Protein Expression and Purification

For the preparation of recombinant proteins: two hundred milliliters of LB culture containing 50 μg/mL of kanamycin or 100 μg/mL of ampicillin in 1 L Erlenmeyer flasks were incubated with a rotary shaking rate of 250 rpm at 37 °C. When the absorbance (A_{600}) reached around 1.0, recombinant protein expression was induced by adding isopropyl-β-D-thiogalactopyranoside (IPTG) to a final concentration of 0.01–0.1 mM. The culture was then incubated at 37 °C for 4 h or at 18 °C for 20 h, depending on enzyme-specific optimum expression conditions. Cells were then harvested by centrifugation at 4 °C, washed twice with 50 mM Tris-HCl buffer (pH 7.5), and re-suspended in 15 mL of 30 mM Tris-HCl buffer

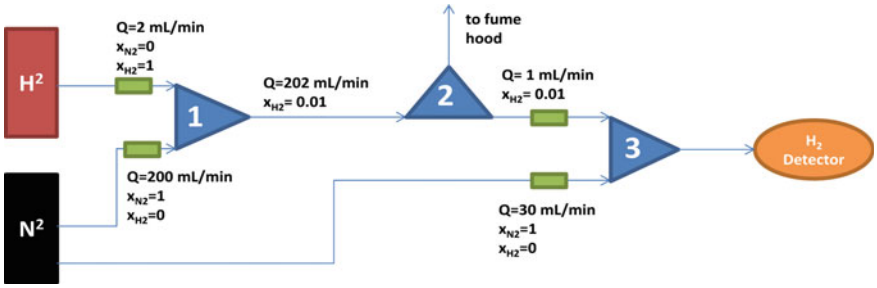

Fig. 3 Flow calibration setup. In this figure green boxes indicate gas flow controllers, and 0.25 in pipe junctions are shown as blue triangles. Pure hydrogen is first mixed with pure nitrogen at junction 1. A subset of this mixture is mixed again with a second stream of pure nitrogen, to yield a total of 30 mL/min gas through the detector. Example flow rates and mass fractions are included above to give a final hydrogen concentration of 330 ppm

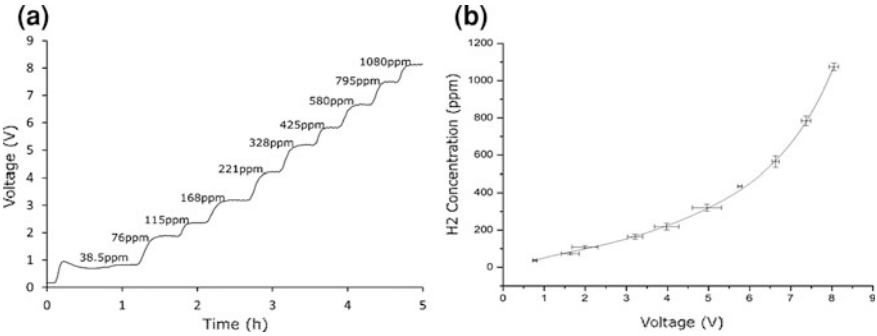

Fig. 4 Example flow calibration (**a**), produced by adjusting the input ratio of pure N_2 and H_2 gases, and calibration curve (**b**), produced from flow calibrations performed in duplicate

(pH 7.5) containing 0.5 M of NaCl and 1 mM of EDTA. Cells were lysed using a Fisher Scientific Sonic Dismembrator Model 500 (5 s pulse on and off, total 360 s, 20 % amplitude) in an ice bath. After centrifugation, the target proteins were purified using several methods, including as His-tag purification, cellulose binding module (CBM) purification followed by intein self-cleavage or ethylene glycol elution, and heat treatment. His-tagged proteins, including G6PDH, 6PGDH, TK, and TAL, were purified using Ni-charged resins (Bio-Rad, Profinity IMAC Ni-Charged Resin). PGM, FBP, PGI, and PPGK were purified by intein self-cleavage or ethylene glycol elution [26–29]. RPI, RPE, TIM, and ALD were purified by heat precipitation conducted at 80 °C for 20 min [30, 31].

3.3 Enzyme Activity Assays

Activity data below include at least one specific activity for each enzyme at 50 °C and/or 60 °C. In the case where one is not listed, a Q10 temperature coefficient of 2 was used for determination of enzyme loading at an uncharacterized temperature.

Thermobifida fusca CBM-PPGK activity was measured based on the generation of glucose 6-phophate from polyphosphate and glucose in a 50 mM HEPES buffer (pH 7.5) containing 4 mM $MgCl_2$, 5 mM D-glucose, and 1 mM polyphosphate at 50 °C for 5 min [28]. The specific activity of CBM-PPGK was 64.6 U/mg at 50 °C.

Geobacillus stearothermophilus G6PDH activity was measured in 100 mM HEPES buffer (pH 7.5) containing 5 mM $MgCl_2$ and 0.5 mM $MnCl_2$, 2 mM glucose 6-phosphate, and 0.67 mM $NADP^+$. The increase in absorbance at 340 nm was measured in 5 min. The specific activity was 35 U/mg at 50 °C [32].

Morella thermoacetica 6PGDH activity was measured in a 50 mM HEPES buffer (pH 7.5) containing 2 mM 6-phosphogluconate, 1 mM $NADP^+$, 5 mM $MgCl_2$, and 0.5 mM $MnCl_2$, at 37 °C for 5 min [32]. The reaction product NADPH was measured at 340 nm. The specific activity was 16 U/mg at 50 °C.

T. maritima RPI activity was assayed by a modified Dische's cysteine–carbazole method. The specific activity was 300 U/mg at 50 °C [30].

T. maritima RPE activity was determined on a substrate D-ribulose 5-phosphate as described previously [33]. The specific activity of RPE was 1.42 U/mg at 50 °C.

T. thermophilus TK activity assay was measured on the substrates of D-xylulose 5-phosphate and D-ribose 5-phosphate. The reactions were carried out in a 50 mM Tris/HCl pH 7.5 buffer containing 0.8 mM D-xylulose 5-phosphate, 0.8 mM D-ribose 5-phosphate, 15 mM $MgCl_2$, 0.03 mM Thiamine pyrophosphate, 0.14 mM NADH, 60 U/mL of TIM, and 20 U/mL of glycerol 3-phosphate dehydrogenase [33]. The specific activity of TK was 1.3 U/mg at 25 °C, or approximately 3.9 U/mg at 50 °C.

T. maritima TAL activity assay was carried out as reported previously. This enzyme had a specific activity of 42 U/mg at 80 °C [34], or 5.25 U/mg at 50 °C.

T. thermophilus TIM activity was measured in 100 mM HEPES pH 7.5 containing 10 mM $MgCl_2$, 0.5 mM $MnCl_2$ at 60 °C for 5 min containing 2 mM D-glyceraldehyde 3-phosphate [35]. The reaction was stopped with $HClO_4$ and neutralized with KOH. The product dihydroxyacetone phosphate was measured by using glycerol 3-phosphate dehydrogenase in the presence of 0.15 mM NADH at 25 °C [35]. The specific activity at these conditions was 870 U/mg at 60 °C.

T. thermophilus ALD was assayed in 100 mM HEPES pH 7.5 containing 10 mM-$MgCl_2$, and 0.5 mM $MnCl_2$ at 60 °C for 5 min with 2 mM of D-glyceraldehyde 3-phosphate in the presence of TIM, FBP, and PGI. The reaction was stopped with $HClO_4$ and neutralized with KOH [35]. The product glucose 6-phosphate was analyzed at 37 °C with a liquid glucose reagent set (Pointe scientific). The specific activity of ALD was 36 U/mg at 60 °C.

T. maritima FBP activity was determined based on the release of phosphate and its specific activity of FBP at 60 °C was 12 U/mg [29].

C. thermocellum PGI activity was assayed at 60 °C in 100 mM HEPES (pH 7.5) containing 10 mM $MgCl_2$ and 0.5 mM $MnCl_2$ with 5 mM fructose 6-phosphate as substrate [27]. After 3 min the reaction was stopped with $HClO_4$ and neutralized with KOH. The product glucose 6-phosphate was analyzed with a liquid glucose hexokinase kit (Pointe scientific). The specific activity of PGI at 60 °C was 1,900 U/mg.

P. furiosus SHI hydrogenase was produced as reported previously [25]. NADPH-based specific activity was 0.8 U/mg at 50 °C.

3.4 Preparation of the Enzyme Cocktail

The reaction buffer contained 100 mM HEPES (pH 7.5), 0.5 mM thiamine pyrophosphate, 10 mM $MgCl_2$, and 0.5 mM $MnCl_2$. For the glucose demonstration experiment, the concentrations of glucose, $NADP^+$, and polyphosphate ($(P_i)_6$, sodium hexametaphosphate) were 2, 4 and 4 mM, respectively. For the high-rate glucose 6-phosphate utilization experiment, the concentrations of glucose 6-phosphate and $NADP^+$ were 100 and 8 mM, respectively. Enzymes were added according to the loadings in Table 2.

To prevent microbial growth, 50 μg/mL of kanamycin was added. Once all other reaction components were combined, substrate was added to start the reaction. The reactor was sealed and magnetic agitation was started, along with nitrogen carrier gas at a flow rate of 30 mL/min. Data acquisition occurred continuously with a TCD. When the oxygen inside the reactor was completely evacuated, the hydrogenase enzymes became uninhibited. Once a sufficient amount of $NADP^+$ was converted to NADPH by the SyPaB pathway, hydrogen production started. During the experiment temperature, carrier gas flow, and hydrogen signal were monitored.

3.5 Other Assays

Soluble protein concentration was measured by the Bio-Rad modified Bradford protein kit with bovine serum albumin as the standard protein. Enzyme molecular weights were verified using 12–15 % SDS-PAGE performed in *Tris*–glycine buffer, as described elsewhere.

4 Hydrogen Production from Glucose via a Synthetic Enzymatic Pathway

To demonstrate the effectiveness of the custom apparatus, hydrogen was generated from glucose. As shown in Fig. 1, in this reaction polyphosphate was used as a phosphate moiety donor, a reaction catalyzed by polyphosphate glucokinase from

Table 2 Enzymes used in hydrogen generation experiments

No.	Enzymes	EC number	Source	Glc loading (U/mL)	G6P loading (U/mL)	References
1	Polyphosphate glucokinase (PPGK)	2.7.1.63	Tfu1811	1	0	[28]
2	Glucose 6-phosphate dehydrogenase (G6PDH)	1.1.1.49	GsG6PDH	1	16	[44]
3	6-phosphogluconate dehydrogenase (6PGDH)	1.1.1.44	Moth1283	1	16	[33]
4	Ribose 5-phosphate isomerase (RPI)	5.3.1.6	Tm1080	1	1.6	[30]
5	Ribulose 5-phosphate 3-epimerase (RPE)	5.1.3.1	Tm1718	1	1.6	[17]
6	Transketolase (TK)	2.2.1.1	Ttc1896	1	1.6	Unpublished data
7	Transaldolase (TAL)	2.2.1.2	Tm0295	1	1.6	[34]
8	Triose phosphate isomerase (TIM)	5.3.1.2	Ttc0581	1	1.6	[33]
9	Fructose bisphosphate aldolase (ALD)	4.1.2.13	Ttc1414	1	1.6	[18]
10	Fructose bisphosphatase (FBP)	3.1.3.11	Tm1415	1	1.6	[29]
11	Phosphoglucose isomerase (PGI)	5.3.1.9	Cthe0217	1	1.6	[27]
12	Hydrogen dehydrogenase (H_2ase)	1.12.1.3	P. furiosus	1	5.6	[25]

The first enzyme loading column is for the proof of concept conversion of glucose, and the second is high-rate production from glucose-6-phosphate

T. fusca (Liao et al. [28]). This kinase is able to use polyphosphate instead of ATP. The product of this reaction, glucose 6-phosphate (g6p), is then oxidized to ribulose 5-phosphate (ru5p) by the action of two dehydrogenases, glucose 6-phosphate dehydrogenase (G6PDH) and 6-phosphogluconolactone (6PGDH), along with the coreduction of $NADP^+$ to NADPH. Pentose phosphate pathway enzymes then convert 6 mol equivalent of ru5p to 5 mol equivalent of g6p. A hydrogenase enzyme completes the cascade, converting NADPH plus free protons to H_2 and recycled $NADP^+$. Equation (1) shows the overall formula for hydrogen production from glucose.

$$C_6H_{12}O_6 + 7H_2O + (HPO_3)_n \rightarrow 12H_2 + 6CO_2 + (HPO_3)_{n-1} + H_3PO_4 \quad (1)$$

The reaction was carried out in 100 mM HEPES buffer (pH 7.5), containing 2 mM glucose, 2 mM polyphosphate, 4 mM $NADP^+$, 10 mM $MgCl_2$, 0.5 mM $MnCl_2$, and 0.5 mM thiamine pyrophosphate. Enzyme loadings were 10 U G6PDH and 6PGDH, and 1 U of all other enzymes. Reactor volume was 1 mL.

The maximum hydrogen generation rate for this reaction was 8.4 mmol H_2 per liter of reactor volume per hour (mmol/L/h) at 50 °C (Fig. 5a). This is over twice the rate observed for previous SyPaB studies conducted at the same substrate loading (2 mM) and similar enzyme loadings. These cases produced maximum

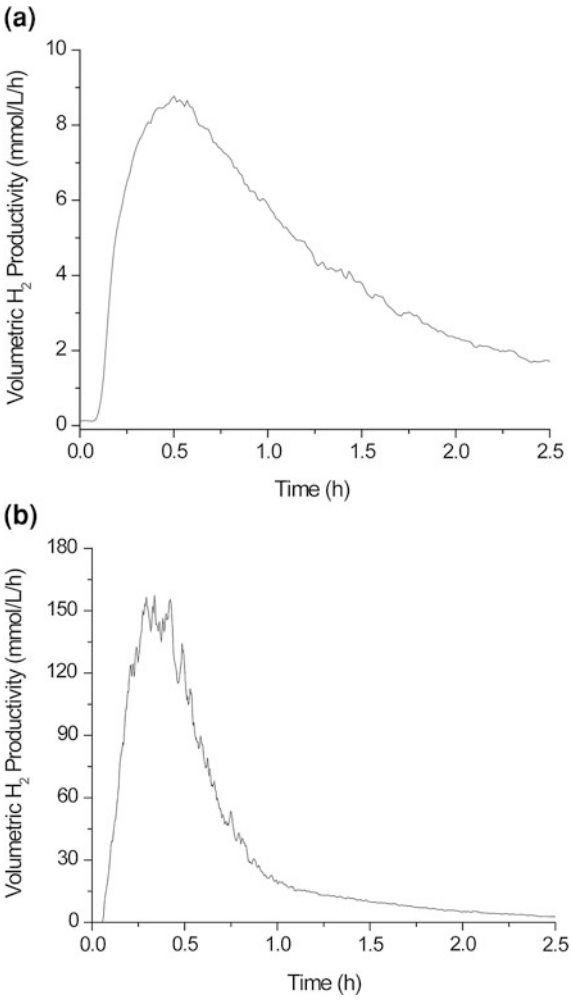

Fig. 5 Production of hydrogen from glucose for the first time (**a**) and high-rate production of hydrogen from glucose-6-phosphate (**b**). The glucose reaction was carried out at is reaction was carried out at 50 °C, with a substrate loading of 2 mM, 4 mM $NADP^+$, and 1 U/mL enzyme loading. The glucose 6-phosphate reaction was conducted at 60 °C, with a substrate loading of 100 mM, 8 mM $NADP^+$, and a high total enzyme loading (Table 2)

rates of 0.44 mmol/L/h from starch at 30 °C [15], 0.72 mmol/L/h from g6p at 30 °C [15], 0.48 mmol/L/h from cellobiose and 3.92 mmol/L/h from cellopentose at 32 °C [16], and 2.2 mmol/L/h from xylose at 50 °C [17].

Another trend apparent among these results is the shape of the curve. Studies with an irreversible phosphorylation reaction (glucose and g6p) as a substrate typically have a sharp peak of initial production, followed by low-level H_2 production for several hours, such as this study and those by Myung et al. [18] and Zhang et al. [15]. Polymeric substrates with a reversible step included in their phosphorylation reaction (i.e., starch) or a long substrate phosphorylation (e.g., xylose) tend to have lower initial peaks, with a period of intermediate H_2 production [15–17]. Production from sucrose, in which half the hexose substrate contains a reversible step, and half of which does not, displays a hybrid profile [18].

5 High-Speed Hydrogen Production from Glucose 6-Phosphate

The rate of hydrogen generation is a primary factor for determining the possible applications for a given technology [36]. Although the rate of 8.4 mmol/L/h observed during the conversion of glucose at 50 °C was higher than the previous maximum rate of 3.92 mmol/L/h [16], higher temperatures and increased substrate concentration, and more enzyme and cofactor loadings offered the potential for additional rate enhancements.

To further increase hydrogen generation rates, we investigated the effects of elevated temperatures, substrate concentration, and key enzyme loadings on the maximum hydrogen generation rate as predicted previously [36]. Most of the enzymes (#2–12) used in the production of hydrogen from glucose are thermostable at temperatures above 50 °C, however #1, PPGK, degrades rapidly above this temperature. For this reason, glucose 6-phoshate was selected as the starting substrate for the high-rate experiments. When more stable phosphorylases or kinases are found or engineered, we expect similar rates will be available from lower-cost substrates as well.

The case where the highest rate of SyPaB hydrogen production was achieved is shown in Fig. 5b. The reaction temperature was increased to 60 °C, the substrate loading was increased to 100 mM glucose 6-phosphate, and the cofactor concentration was increased to 8 mM. Enzyme loadings were increased as summarized in Table 2, where the total reaction volume was 1 mL. The maximum hydrogen rate was 157 mmol/L/h, one of the highest biohydrogen generation rates reported [37]. This reaction rate can be compared to well-known fermentations using a power output per unit volume basis. Examining the maximum hydrogen production rate on the basis of combustible energy produced, 157 mmol H_2/L/h is equivalent to 12.5 W/L, already approaching the energy productivity of a highly mature bioprocess, ethanol fermentation, which is typically 16–30 W/L [38]. In the past decade, SyPaB hydrogen generation has been increased from 0.21 to 157 mmol of H_2 per liter per hour, an improvement of approximately 750-fold. Note that NADP is not stable at 60 °C, resulting in a hydrogen yield lower than the theoretical yield. Therefore, it is essentially important to replace NADP with low-cost and stable biomimetic cofactors in the future [39].

6 Large-Scale Hydrogen Production Bioreactor

The use of purified enzymes simplifies bioreactor design challenges in several regards. Without cell membranes, a major barrier is eliminated in the transport of substrates and products, enabling faster reaction rates, as well as easier sampling and better engineering control [39]. When thermoenzymes are used, higher temperatures may be used, which enable still faster reaction rates, without the difficulties associated with thermophile fermentation. Thermoenzymes also enable the

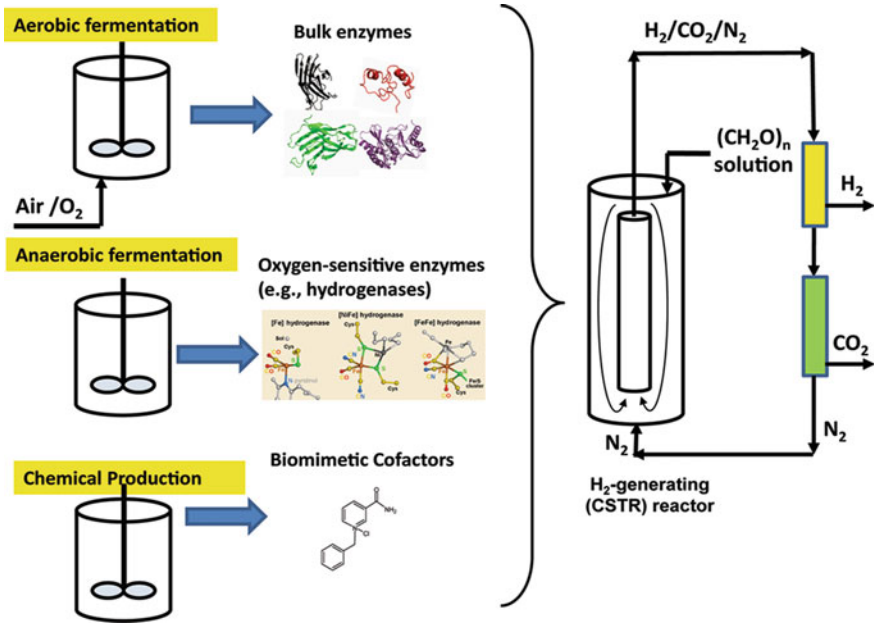

Fig. 6 Reactor systems used for large-scale hydrogen production, including the preparation of enzymes and biomimetic cofactor, continuous hydrogen production in an air-lifted CSTR, and membrane reactors for product separation

possibility of immobilization in a much simpler manner than is possible for microbial systems [40]. Significantly, enzymatic hydrogen production by SyPaB is an endothermic, exergonic reaction [15]. This means heat transfer from nearby operations may be used effectively to upgrade waste heat from air conditioners, refrigerators, and fuel cells to chemical energy H_2, resulting in unmatched thermal conversion efficiency. The challenges that remain for cell-free hydrogen are primarily oxygen and product inhibition, which drive the requirement for an anaerobic reactor with in situ product removal.

In order for biocommodities to be produced economically using in vitro methods, industrial-scale reactors must be employed. Primary concerns at the laboratory scale revolve around elimination of oxygen, temperature control, stable pH, product removal, and easy access, however, factors such as cost and homogeneity become equally important when scaling up. The most common method of minimizing cost and ensuring homogeneity in industrial bioprocesses is to develop continuous methods; a similar alternative is fed-batch, which may be considered a continuous process for periods of time in systems such as enzymatic hydrogen generation, where soluble biocatalysts, cofactors, and reaction buffer are the only components that are not added or removed.

A general proposed flow diagram for fed-batch SyPaB hydrogen generation is presented as Fig. 6. This scheme, although similar to that proposed by Swartz [41], has key differences: in this case the enzymatic hydrogen production occurs in the

absence of oxygen, and different bioreactors are used to produce different enzymes instead of one due to different growth conditions. Here there are three biocatalyst sources: anaerobic fermentation for producing oxygen-sensitive enzymes such as hydrogenases; aerobic fermentation for producing most enzymes, such as #1–11; and synthetic chemical production of cofactors. Biomimetic cofactors such as the example molecule shown provide increased thermostability and reduced cost [39].

Selective separation of gaseous products from the carrier gas stream is necessary for continuous operation (Fig. 6) as a pair of membrane separation units; these may also be combined into a single step with the reactor [42], although this may incur additional cost. More complex configurations may also be considered, in order to achieve certain goals. For example, modeling by Ardao and Zeng [43] suggested that SyPaB hydrogen production would benefit from separation of the hydrogenase and other reactions, in order to capitalize on the higher hydrogenase activity at higher temperatures.

7 Conclusions

In summary, a new system for hydrogen generation and detection was constructed, calibrated, and tested. Novel reactor design allowed precise control of the liquid phase, prevented oxygen contamination, and ensured the system was well-mixed and held at a constant temperature, and had a constant volume. A flow calibration system was used to avoid inaccuracies associated with electrolysis-based calibration calculations. Hydrogen generated from glucose represents the first time monomer hexose sugars were utilized by a SyPaB reaction. Finally, engineering principles were used to increase the maximum volumetric hydrogen production rate to 157 mmol/L/h, a rate sufficient for industrial implementation of this technology.

Acknowledgments This work was supported by the Defense University Research Instrumentation Program (DURIP), Shell GameChanger Program, the CALS Biodesign and Bioprocessing Research Center to PZ at Virginia Tech, as well as two NSF STTR I (IIP–1321528) and DOE STTR I (DE-SC0009659TDD) awards to Cell Free Bioinnovations Inc. JR was supported by the Department of Defense through the National Defense Science and Engineering Graduate (NDSEG) Program. MA was supported by the Division of Chemical Sciences, Geosciences and Biosciences, Office of Basic Energy Sciences of the US Department of Energy (grant DE-FG05-95ER20175).

References

1. Lipman T (2011) An overview of hydrogen production and storage systems with renewable hydrogen case studies. Clean Energy States Alliance
2. Ramachandran R, Menon RK (1998) An overview of industrial uses of hydrogen. Int J Hydrogen Energy 23:593–598
3. Ramage MP, Agrawal R (2004) The hydrogen economy: opportunities, costs, barriers and R&D needs. National Research Council of the National Academies, p 15

4. Zhang Y-HP (2013) Next generation biorefineries will solve the food, biofuels, and environmental trilemma in the energy-food-water nexus. Energy Sci Eng 1:27–41
5. Daugherty R (2013) Cost effective distributed hydrogen production systems. VT KnowledgeWorks Strategic Services Division
6. Das D, Veziroğlu TN (2001) Hydrogen production by biological processes: a survey of literature. Int J Hydrogen Energy 26:13–28
7. Hawkes F, Dinsdale R, Hawkes D, Hussy I (2002) Sustainable fermentative hydrogen production: challenges for process optimisation. Int J Hydrogen Energy 27:1339–1347
8. Argun H, Kargi F (2011) Bio-hydrogen production by different operational modes of dark and photo-fermentation: an overview. Int J Hydrogen Energy 36:7443–7459
9. Ducat DC, Sachdeva G, Silver PA (2011) Rewiring hydrogenase-dependent redox circuits in cyanobacteria. Proc Nat Acad Sci U.S.A 108:3941–3946
10. Wang J, Wan W (2009) Factors influencing fermentative hydrogen production: a review. Int J Hydrogen Energy 34:799–811
11. Enfors S-O, Jahic M, Rozkov A, Xu B, Hecker M, Jürgen B, Krüger E, Schweder T, Hamer G, O'beirne D (2001) Physiological responses to mixing in large scale bioreactors. J Biotechnol 85:175–185
12. Van Groenestijn J, Hazewinkel J, Nienoord M, Bussmann P (2002) Energy aspects of biological hydrogen production in high rate bioreactors operated in the thermophilic temperature range. Int J Hydrogen Energy 27:1141–1147
13. Woodward J, Mattingly SM, Danson M, Hough D, Ward N, Adams M (1996) In vitro hydrogen production by glucose dehydrogenase and hydrogenase. Nat Biotechnol 14:872–874
14. Woodward J, Orr M, Cordray K, Greenbaum E (2000) Biotechnology: enzymatic production of biohydrogen. Nature 405:1014–1015
15. Zhang Y-HP, Evans BR, Mielenz JR, Hopkins RC, Adams MWW (2007) High-yield hydrogen production from starch and water by a synthetic enzymatic pathway. PLoS ONE 2:e456
16. Ye X, Wang Y, Hopkins RC, Adams MWW, Evans BR, Mielenz JR, Zhang YHP (2009) Spontaneous high-yield production of hydrogen from cellulosic materials and water catalyzed by enzyme cocktails. ChemSusChem 2:149–152
17. del Martin Campo JS, Rollin J, Myung S, You C, Chandrayan S, Patino R, Adams MWW, Zhang YHP (2013) High-yield production of dihydrogen from xylose by using a synthetic enzyme cascade in a cell-free system. Angew Chem Int Ed 125:4685–4688
18. Myung S, Rollin JA, You C, Sun F, Chandrayan S, Adams MWW, Zhang Y-HP (2014) In vitro metabolic engineering of hydrogen production at theoretical yield from sucrose. Metab Eng Epub:10.1016/j.ymben.2014.1005.1006
19. Iwuchukwu IJ, Vaughn M, Myers N, O'Neill H, Frymier P, Bruce BD (2009) Self-organized photosynthetic nanoparticle for cell-free hydrogen production. Nat Nanotech 5:73–79
20. Millsaps JF, Bruce BD, Lee JW, Greenbaum E (2001) Nanoscale photosynthesis: photocatalytic production of hydrogen by platinized photosystem I reaction centers. Photochem Photobiol 73:630–635
21. Zhang Y-HP (2010) Renewable carbohydrates are a potential high-density hydrogen carrier. Int J Hydrogen Energy 35:10334–10342
22. Krassen H, Schwarze A, Friedrich Br, Ataka K, Lenz O, Heberle J (2009) Photosynthetic hydrogen production by a hybrid complex of photosystem I and [NiFe]-hydrogenase. ACS Nano 3:4055–4061
23. Wu J, Upreti S, Ein-Mozaffari F (2013) Ozone pretreatment of wheat straw for enhanced biohydrogen production. Int J Hydrogen Energy 38(25):10270–10276
24. Figaro (2004) TGS 821—special sensor for hydrogen gas product information. Figaro USA Inc
25. Chandrayan SK, McTernan PM, Hopkins RC, Sun JS, Jenney FE, Adams MWW (2012) Engineering hyperthermophilic archaeon *Pyrococcus furiosus* to overproduce its cytoplasmic NiFe–hydrogenase. J Biol Chem 287:3257–3264

26. Wang Y, Zhang Y-HP (2010) A highly active phosphoglucomutase from *Clostridium thermocellum*: cloning, purification, characterization, and enhanced thermostability. J Appl Microbiol 108:39–46
27. Myung S, Zhang X-Z, Zhang Y-HP (2011) Ultra-stable phosphoglucose isomerase through immobilization of cellulose-binding module-tagged thermophilic enzyme on low-cost high-capacity cellulosic adsorbent. Biotechnol Prog 27:969–975
28. Liao HH, Myung S, Zhang Y-HP (2012) One-step purification and immobilization of thermophilic polyphosphate glucokinase from *Thermobifida fusca* YX: glucose-6-phosphate generation without ATP. Appl Microbiol Biotechnol 93:1109–1117
29. Myung S, Wang Y, Zhang Y-HP (2010) Fructose-1, 6-bisphosphatase from a hyper-thermophilic bacterium *Thermotoga maritima*: characterization, metabolite stability, and its implications. Process Biochem 45:1882–1887
30. Sun FF, Zhang XZ, Myung S, Zhang Y-HP (2012) Thermophilic *Thermotoga maritima* ribose-5-phosphate isomerase RpiB: optimized heat treatment purification and basic characterization. Protein Expr Purif 82:302–307
31. Myung S, Zhang Y-HP (2013) Non-complexed four cascade enzyme mixture: simple purification and synergetic co-stabilization. PLoS ONE 8:e61500
32. Zhu ZG, Sun F, Zhang X, Zhang Y-HP (2012) Deep oxidation of glucose in enzymatic fuel cells through a synthetic enzymatic pathway containing a cascade of two thermostable dehydrogenases. Biosens Bioelectron 36:110–115
33. Wang Y, Huang W, Sathitsuksanoh N, Zhu Z, Zhang Y-HP (2011) Biohydrogenation from biomass sugar mediated by in vitro synthetic enzymatic pathways. Chem Biol 18:372–380
34. Huang SY, Zhang Y-HP, Zhong JJ (2012) A thermostable recombinant transaldolase with high activity over a broad pH range. Appl Microbiol Biotechnol 93:2403–2410
35. You C, Myung S, Zhang Y-HP (2012) Facilitated substrate channeling in a self-assembled trifunctional enzyme complex. Angew Chem Int Ed 51:8787–8790
36. Zhang Y-HP (2011) Simpler is better: high-yield and potential low-cost biofuels production through cell-free synthetic pathway biotransformation (SyPaB). ACS Catal 1:998–1009
37. Rittmann S, Herwig C (2012) A comprehensive and quantitative review of dark fermentative biohydrogen production. Microb Cell Fact 11:115
38. Querol A, Fleet GH (eds) (2006) The yeast handbook: yeasts in food and beverages. Springer, Berlin
39. Rollin JA, Tam W, Zhang YP (2013) New biotechnology paradigm: cell-free biosystems for biomanufacturing. Green Chem 15:1708–1719
40. Myung S, You C, Zhang YP (2013) Recyclable cellulose-containing magnetic nanoparticles: immobilization of cellulose-binding module-tagged proteins and synthetic metabolon featuring substrate channeling. J Mater Chem B 15:1708–1719
41. Swartz JR (2013) SBE supplement: biochemical engineering—cell-free bioprocessing. In: Chemical engineering progress. American Institute for Chemical Engineers, New York, USA
42. Prazeres D, Cabral J (1994) Enzymatic membrane bioreactors and their applications. Enzyme Microb Technol 16:738–750
43. Ardao I, Zeng A-P (2013) In silico evaluation of a complex multi-enzymatic system using one-pot and modular approaches: application to the high-yield production of hydrogen from a synthetic metabolic pathway. Chem Eng Sci 87:183–193
44. Zhu Z, Tam TK, Sun F, You C, Zhang Y-HP (2014) A high-energy-density sugar biobattery based on a synthetic enzymatic pathway. Nat Commun 5:3026